

# Comparative Evaluation of Denoising of Tree Radar B-scan Images Using Multi-resolution Analysis Algorithms

Zhaoxi Li, Jian Wen\*, Zhongliang Xiao, and Mingkai Wang

**Abstract**—This paper uses Ground Penetrating Radar (GPR) to detect the decays in the tree trunk such as decay, scar, void, etc. The noise submerges the feature information of the defects, which lead to inaccurate or even incorrect results. This paper focuses on multi-resolution algorithms, which serve to improve the signal to noise ratio (SNR) of tree radar B-scan images, and extract the edge feature information of defects. The performance of these algorithms will be compared in PSNR and EPI (edge preservation index). The experiments carried on the simulated tree radar data which is obtained by GprMAX based of FDTD (Finite-Difference Time-Domain) and the actual willow radar data which is obtained by TRU tree radar detect system. This paper also presents the results of forward tree radar B-scan image and reality tree radar B-scan image.

**Keywords**—edge preservation index, multi-resolution algorithm, signal to noise ratio, tree radar B-scan image.

## I. INTRODUCTION

GROUND Penetrating Radar (GPR), as an effective non-destructive testing technology, has been gradually applied to the NDT of trees [1-3]. However, due to the noise, there are problems such as low signal-to-noise-ratio and inconspicuous defect features in the tree radar B-scan images [4]. There are lots of noise filtering algorithms presented in the literature. Traditional denoising techniques can only effectively remove noise. However, for the tree radar wave image, the curve characteristic of the defect inside the tree is the most important information. Therefore, it is an algorithm suitable for the tree radar wave image that can effectively remove the noise while maintaining the edge feature of the defect. The multi-resolution geometric analysis algorithm has good directional selectivity and can effectively extract the edge

features of the image [5-7].

The commonly used multi-resolution analysis algorithms mainly include Wavelet transform, Curvelet transform, Contourlet transform and Shearlet transform. In the recent years, Wavelet transform has been applied to remove noise from signals and images. Goyal applied the continuous Wavelet transform to the gravity and magnetic data to estimate the thickness of sub-basalt sediment. The research shows that the satisfactory results for the synthetic and real data case study support the application of the continuous Wavelet transform technique [8]. Kumar et al used the discrete Wavelet transform to measure outer race defect width of taper roller bearing in the vibration signal. The result indicates that the discrete Wavelet transform is suitable for measuring outer race defect width of taper roller bearing. Compared with the traditional image removal noise technology, Wavelet transform has achieved good results in the above research [9]. However, for two-dimensional data images, the main information in the imagers is its edge features, and the Wavelet transform performs poorly in the edge feature retention ability of the image due to its poor direction information extraction capability. To overcome this shortcoming of Wavelet transform and to process high-dimensional image more efficiently, the Curvelet transform has been developed to eliminate the noise from images and signals. Cieszczyk presents the application of Curvelet transform to the analysis of GPR images received from synthetic and experimental data of concrete. The results show that the application of Curvelet transform to B-scan images with many disturbances, like air bubbles, can properly eliminate most of the visual artifacts and recover more details from the image [10]. Tzanis uses the discrete Curvelet transform to perform noise removal processing on the GPR data image to recover the directional scale and other information contained in the 2D radar data. The research indicates that the Curvelet transform offers a provably effective and powerful method to process and analysis noisy and complex data [11]. Terrasse et Al utilized the ground penetrating radar to detect the underground buried pipe and used the Curvelet transform to remove the clutter and noise from the GPR scan image. The position of the buried pipe can be accurately located [12]. Above research shows the Curvelet transform has effective performance on removing noise from image or signal. Because the Curvelets are highly anisotropic and provide sparse

This research is financially supported by the National Natural Science Foundations of China (Grant No.31600588 and Grant No.31600589) and the Fundamental Research Funds for the Central Universities (NO.2015ZCQ-GX-01, NO. 2017ZY27). The authors have no conflict of interest to declare.

Zhaoxi Li, with Beijing Forestry University, Beijing, 100083 China (e-mail: lizhaoxi14@163.com).

Jian Wen, with Beijing Forestry University, Beijing, 100083 China (corresponding author to provide e-mail: [wenjian@bjfu.edu.cn](mailto:wenjian@bjfu.edu.cn)).

Zhongliang Xiao, with Beijing Forestry University, Beijing, 100083 China (e-mail: xzliang@126.com).

Mingkai Wang, with Beijing Forestry University, Beijing, 100083 China (corresponding author to provide e-mail: [misslittlesheep@163.com](mailto:misslittlesheep@163.com)).

representation of functions with singularities on curves. However, the discretization of Curvelet transform is difficult to achieve. Inheriting the directional selectivity of the Curvelet transform, the Contourlet transform has been proposed to remove noise from image and signal and has been widely used in image or signal de-noising domain. Satheesh applies the Contourlet transform to remove the Gaussian noise from MR Images. It is found that the Contourlet transform outperforms the Wavelet transform methods both visually and in terms of PSNR [13]. Qing Guo et al applied the Contourlet transform to remove noise for optical coherence tomography heart tube image. Compared with the Wavelet and Curvelet transform, the Contourlet transform achieves better denoising results [14]. The Curvelet and Contourlet transforms subdivide the images in the frequency domain, which will affect the sparse representation of the images to some extent. Therefore, the Shearlet transform has been constructed using a special form of affine system on the basis of Wavelet transform theory and multi-resolution geometric analysis theory. Shearlet transform can accurately represent high-dimensional signals in terms of scale, direction, and location. Moreover, Shearlet transform has the characteristic of tight support in the frequency domain, and therefore has a strong direction selectivity. Ye Yuan et al uses the Shearlet transform to de-noise the SAR image. The experimental results show that the Shearlet transform outperformed the other method such as enhanced Lee filter, Wavelet transform [15]. Wang Xiannan et al uses the Shearlet transform to perform noise removal processing on the ground-penetrating radar data image. The research verifies the effectiveness and usability of the Shearlet transform in geo-radar wave image [16]. Compared with the traditional noise removal algorithm and Wavelet transform, the Shearlet transform has better noise removal effect.

The aim of this paper is to find the optimal algorithm to remove noise from tree radar B-scan images. The scope of this paper is limited to denoising using various algorithms such as Wavelet, Curvelet, Contourlet and Shearlet transform.

## II. METHODS AND MATERIALS

### A. Wavelet Transform

Wavelet has been used to suppress noise in several investigations. This method decomposes the signal into series of Wavelet coefficients. When the selected signal is more similar to the Wavelet function, the Wavelet coefficients are larger. The random noise usually differs from the Wavelet function, the Wavelet coefficients of noise are smaller. The Wavelet transform is defined as:

$$Wf(a,b) = \langle f, \psi_{ab} \rangle = \int_R f(t) \overline{\psi_{ab}(t)} dt = \int_{-\infty}^{\infty} f(t) \frac{1}{\sqrt{a}} \overline{\psi\left(\frac{t-b}{a}\right)} dt \quad (1)$$

Equation (1) is the continuous Wavelet transform. Where,  $a$ ,  $b$  denote the scale factor and the panning factor respectively. However, due to the scale factor and the panning factor of the

continuous Wavelet transform, there is a large correlation among the Wavelet basis functions, so the Wavelet coefficients are redundant. In order to overcome the shortage, the discrete Wavelet transform is proposed. The realization of discrete Wavelet transform is mainly to limit scale factor and panning factor in the Wavelet basis function to some discrete points. The scale factor is denoted as  $a_0^j$ , and the panning factor is denoted as  $a_0^j k$ , so the discrete Wavelet transform is defined as:

$$Wf(j,k) = a_0^{-j/2} \int_{-\infty}^{\infty} f(t) \overline{\psi(a_0^{-j}t - k)} dt, \quad (2)$$

The discrete Wavelet transform is a multi-resolution analysis method, it decomposes the signal as the Fig.1.

In the Fig.1, the  $S$  represents the raw signal. The  $A1$  is the low frequency sub-band and the  $D1$  is the high frequency sub-band of the first decomposition of  $S$ . Then the low frequency sub-bands of the raw signal are continuously decomposed until the final scale. With the series of decomposition of raw signal  $S$ ,

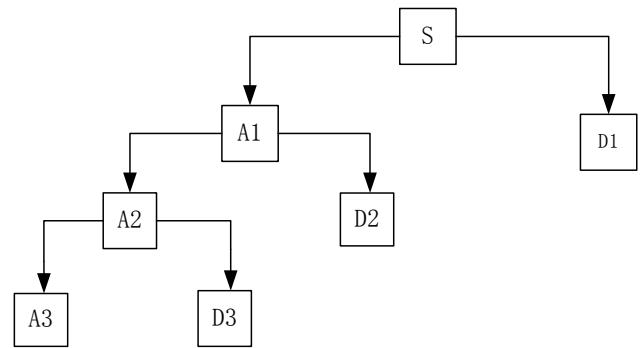


Fig. 1 Multi-resolution decomposition of Wavelet transform

sub-bands decomposition is obtained and threshold processing can be applied to respective bands. Then, the high frequency sub-bands subjected to the threshold processing and the final scale low frequency sub-bands are reconstructed to restore the raw signal which has been removed the noise [17].

### B. Curvelet Transform

The Curvelet transform uses the inner product of the basic function and the signal to achieve a sparse representation of the signal. The inner product is defined as:

$$c(j,l,k) = \left[ f, \varphi_{j,l,k} \right] \quad (3)$$

Where,  $\varphi_{j,l,k}$  is the Curvelet function. Curvelet transform is implemented in the frequency domain by a window function

$U_j$  that is jointly supported by the radial window function  $W(r)$  and the angular window function  $V(t)$ . So the basic Curvelet is defined in polar coordinates as:

$$U_j(r, \theta) = 2^{-3j/4} W(2^{-j} r) V\left(\frac{2^{\lfloor j/2 \rfloor} \theta}{2\pi}\right) \quad (4)$$

Where  $\lfloor j/2 \rfloor$  is the integer part of  $j/2$ . The decomposition of the Curvelet transform in the frequency domain is shown in Fig.2(A).

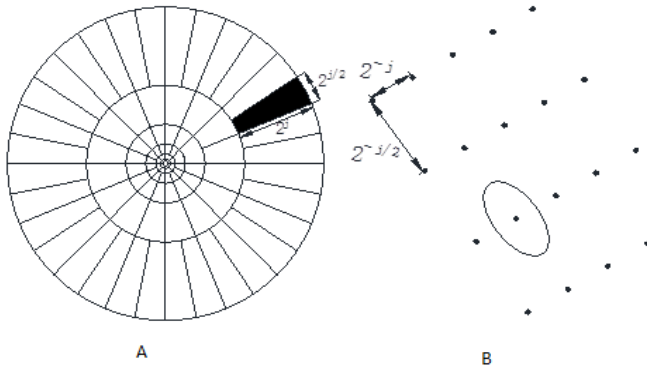


Fig. 2 (A) Decomposition of continuous Curvelet transform in frequency domain, (B) Decomposition of continuous Curvelet transform in spatial domain.

From the Fig.2(A), it can be seen that when the scale  $j$  increases, the second ring increases double so that the width of the edges is proportional to the square of their length. This scale feature is called a parabolic scale. This gives the Curvelet transform better direction selectivity.

However, the formulation of the continuous Curvelet transform is not suitable for Cartesian coordinate. So, the inventors of the Curvelet transform developed the discrete Curvelet transform. In this formulation, the circular coroneae is replaced by rectangular and the rotation of continuous Curvelet transform is replaced by shearing. Therefore, the signal is decomposed in frequency domain by discrete Curvelet transform as Fig.3. In Cartesian coordinate system, the basic Curvelet is defined as:

$$\overline{U}_j(\omega) = \overline{W}_j(\omega) \overline{V}_j(S_{\theta_l} \omega) \quad (5)$$

Where

$$S_{\theta_l} = \begin{pmatrix} 1 & 0 \\ -\tan \theta_l & 1 \end{pmatrix} \quad (6)$$

is the shear matrix. The angles  $\theta_l$  is not equi-spaced but the slops of those angles are equi-spaced. So, the discrete Curvelet transform is defined as:

$$c^D(j, l, k) = \int f(\omega) \overline{U}_j(S_{\theta_l}^{-1} \omega) e^{i(S_{\theta_l}^T b, \omega)} d\omega \quad (7)$$

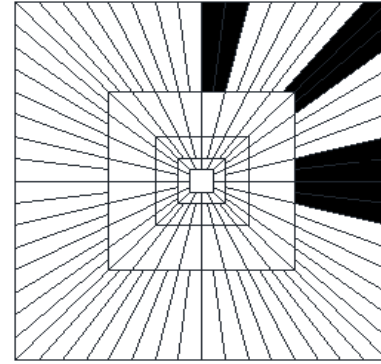


Fig. 3 Decomposition of discrete Curvelet transform in frequency domain

### C. Contourlet Transform

The Contourlet transform is a combination of a Laplacian pyramid filter and a directional filter banks. It is a multi-resolution, multi-directional denoising algorithm. The multi-resolution property is ensured by the Laplacian pyramid filter. It decomposes the image to a low frequency sub-band and a high frequency sub-band on each decomposition level. On the subsequent decomposition level, the low frequency sub-band is decomposed iteratively to obtain the sub-bands of the next decomposition level until the final scale  $n$ . As a result, the image is decomposed into  $n+1$  sub-bands. Which consists of a low frequency sub-band and  $n$  high frequency sub-bands.

The directional property is ensured by the directional filter banks. The directional filter works well in the exact direction information of image in high frequency but poorly in low frequency. The high frequency sub-band comprises the edge detail information of the image. Therefore, the direction filter banks can preserve the useful edge information of the image.

The Contourlet transform combines the advantages of the two filters. It uses the Laplacian filter to decompose the image and uses the directional filter banks to extract detail information [18]. The implementation process is shown in the Fig.4.

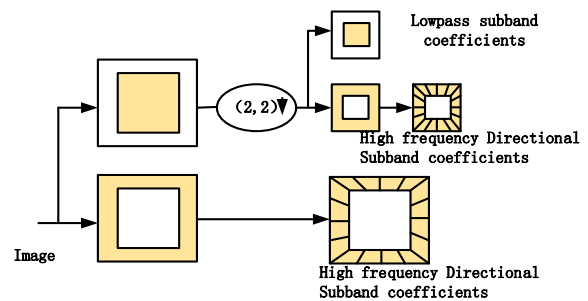


Fig. 4 Decomposition of Contourlet transform

Fig.4 shows us that the Contourlet transform decomposes the image into a low frequency sub-band coefficient and a series of high frequency directional sub-band coefficients. The

directional information is concentrated on the limited transform coefficients in high frequency, so the value of those coefficients is high. However, the noise is evenly distributed across sub-bands. The value of the noise coefficients is low. Therefore, threshold processing can be applied to remove the noise of the image.

*D. Shearlet Transform*

Shearlet transform is a multi-resolution geometric analysis method based on affine system theory. The affine system with synthetic expansion takes the form as:

$$A_{AS}(\psi) = \left\{ \psi_{j,l,k}(x) = |\det A|^{j/2} \psi(S^l A^j x - k) : j, l \in Z, k \in Z^2 \right\} \quad (8)$$

Where,  $\psi \in L2(R2)$ , A and S are both the 2-D invertible matrices .A is the retractable matrix and the S is the shear matrix, of which the modulus value is 1. The matrix A and S are presented as:

$$A = \begin{pmatrix} a & 0 \\ 0 & \sqrt{a} \end{pmatrix}, S = \begin{pmatrix} 1 & s \\ 0 & 1 \end{pmatrix}. \quad (9)$$

The matrix A ensures that the frequency support of the Shearlets becomes increasingly stretched at finer scale and the matrix S controls only the direction of the Shearlets. The different values of a, s support the size of the Shearlets, which is shown in Fig.5(a) in frequency domain [19].

Fig.5(a) is the partition structure of Shearlet transform in frequency. Part C1 and C3 indicate the horizontal area. Part C2 and C4 indicate the vertical area. A pair of wedge areas in

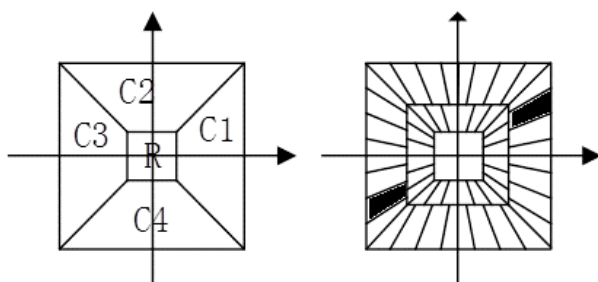


Fig. 5 Discrete Shearlet frequency domain subdivision.

Fig.5(b) are the basic function of C1 and C3.

The steps of denoising by Shearlet transform is following:

Applying Shearlet transform to decompose the image into a final scale low-frequency coefficient and a series of respective scale high-frequency coefficients.

Decomposing the high-frequency coefficients in different orientations and scale by Shearlet window function.

Applying the threshold processing to the decomposed coefficients.

Reconstructing and summing the threshold processed high frequency coefficients sub-bands to obtain the high frequency coefficients.

Synthesizing the processed high frequency coefficients and low frequency coefficients to retire the image.

The Shearlet transform has a strong directionality. When the Shearlet direction is the same as the image information direction, the Shearlet coefficients is large. The Shearlet coefficients of Gaussian white noise is small because of non-directionality. Therefore, the noise coefficients can be suppressed by corresponding threshold function.

*E. Threshold Function*

Threshold is very important for denoising methods. The threshold of this paper is the VisuShrink Threshold. It is also named as universal threshold. This threshold is obtained on the basis of a multidimensional independent normal distribution variable decision theory under the Gaussian noise model. The threshold is defined as:

$$\lambda = \sigma_n \sqrt{2 \ln N} \quad (10)$$

Where, the  $\sigma_n$  is the standard deviation of Gaussian white noise of which the mean is zero. And the N is the length of signal [20].

The threshold function is a function which adopts different processing between coefficients higher than the threshold and coefficients lower than the threshold. There are two kinds of threshold functions: hard threshold function and soft threshold function [21]. If the coefficients are lower than the threshold, it will be removed. The difference between the two functions is that the processing of the coefficients is higher than the threshold. The hard threshold function preserves the coefficients higher than the threshold directly, but the soft threshold function subtracts the threshold then retains. The function images of hard threshold function and soft threshold

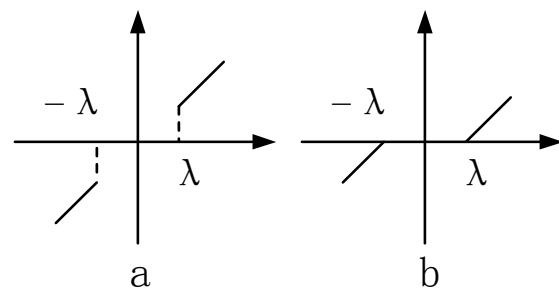


Fig. 6 (a) Hard threshold function image, (b) Soft threshold function image.

function are shown in Fig.6.

The  $\lambda$  in Fig.6 is the threshold. This paper uses the soft threshold function for denoising methods.

III. EXPERIMENTAL RESULTS AND ANALYSIS

To evaluate the performance of those denoising methods, this paper chose a forward tree radar B-scan image for illustration, and then real tree radar B-scan image is used. In addition to visual observations, this paper used the Peak Signal to Noise Ratio (PSNR) [22] and Edge Preservation Index (EPI) [23] as performance measures for denoising. The PSNR is the most commonly used as a measure of quality of reconstruction in image denoising. The EPI is used as the evaluation index of edge preservation ability of image. The mathematical representation of PSNR is presented as:

$$PSNR = 20 \cdot \log_{10} \left\{ \frac{\max(\text{rawData}^2(i, j))}{\sqrt{MSE}} \right\} \quad (11)$$

Where MSE is the mean standard error of de-noised image. The mathematical representation of MSE is presented as:

$$MSE = \frac{\sum_{i=1}^{i=N} \sum_{j=1}^{j=M} (\text{proData}^2(i, j) - \text{rawData}^2(i, j))}{M \times N} \quad (12)$$

The rawData represents the original image data and the proData represents the de-noised image data. The mathematical representation of EPI is shown as:

$$EPI = \sum_i \sum_j \frac{|I_{pro}(i, j+1) - I_{pro}(i, j)|}{|I_{raw}(i, i+1) - I_{raw}(i, j)|} \quad (13)$$

The Fig.3(a) is a model of a simulated tree. There are three defects in (its) trunk. They are scar A, decay B and void C. The forward tree radar B-scan image of this mode tree is shown in Fig.4(b). In the B-scan image, every decay has its own curve characteristics.

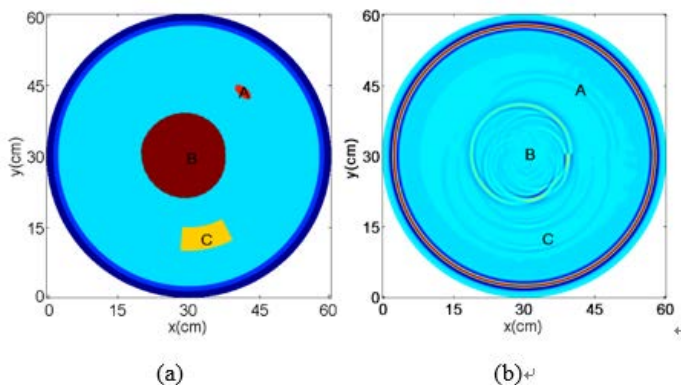


Fig. 7 (a)Forward tree model, (b) Forward tree radar scan.

However, the real B-scan image of tree is easily disturbed by noise. Therefore, in order to simulate the real B-scan image, this paper adds the Gaussian White noise to the forward B-scan

image. The noised image is shown in FIGURE 5.As can be seen from Fig.6, lots of the curve characteristics of the defect are submerged by noise.

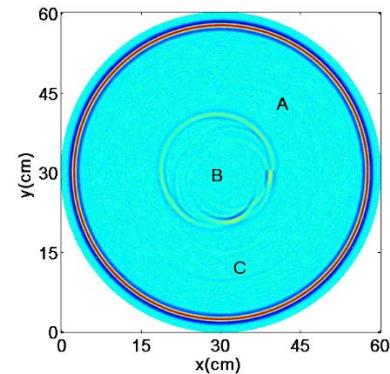


Fig. 8 Noisy forward radar B-scan image.

In order to remove the noise and extract the curve characteristics from the noised B-scan image, this paper applies above four de-noising methods to it. The denoising effect images are shown in Fig.7.

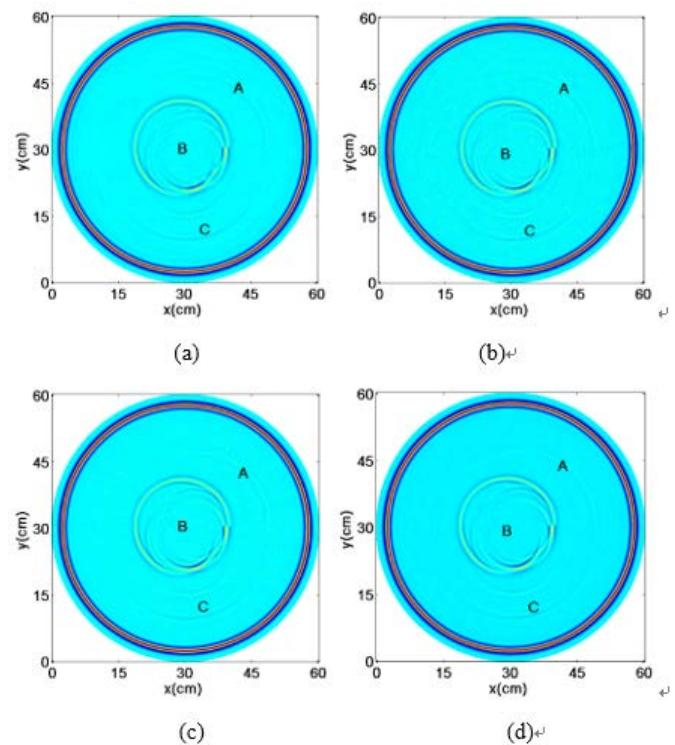


Fig. 9 (a) Wavelet transform denoising effect diagram, (b) Curvelet transform denoising effect diagram, (c) Contourlet transform denoising effect diagram, (d) Shearlet transform denoising effect diagram.

From Fig.8, it is observed that all these denoising algorithms have good denoising effects. The important edge features of these defects are extracted from the noised B-scan image, especially by the Shearlet transform. The Fig.9(d) is the effect image of Shearlet transform. It is observed that the curve characteristics of defects are very obvious. In order to compare the denoising effects of Wavelet, Curvelet, Contourlet and

Shearlet transform, the difference images between the original noised B-scan image and the after de-noised B-scan image of all denoising algorithms are shown in Fig.10.

The Fig.11 is the image of the noise which is added into the forward B-scan image. If the difference image is more like the noise image, the performance of the denoising method is better.

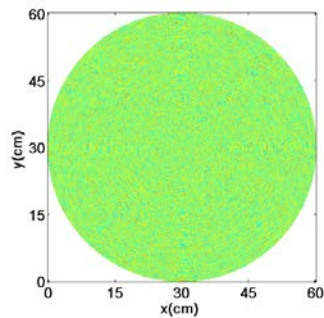


Fig. 10 Noise image.

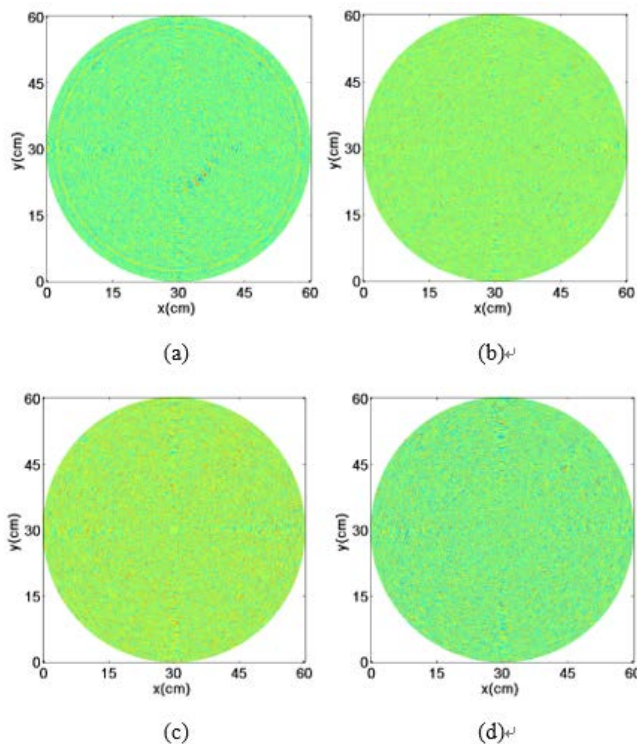


Fig. 11 (a) Wavelet transform denoising effect diagram, (b) Curvelet transform denoising effect diagram, (c) Contourlet transform denoising effect diagram, (d) Shearlet transform denoising effect diagram.

Fig.12(a) is the difference map of the Wavelet transform. There are some curve characteristics of the void in the image, and it indicates when the Wavelet transform removes the noise, the characteristics of defects are lost at the same time. The other difference images don't comprise the characteristics of defects. Especially, the difference image of Shearlet transform is very like the noise image. In other words, the Shearlet transform may be the best algorithm for denoising on forward tree radar B-scan

image.

In order to further evaluate the denoising effects of above denoising algorithms, the PSNR and EPI have been counted and shown in Table 1.

Table 1: The digital results of 4 denoising methods in forward radar B-scan image data.

	Wavelet	Curvelet	Contourlet	Shearlet
PSNR	65.1553	66.8162	66.3513	68.4410
EPI	0.0884	0.2266	0.2962	0.3222

It is observed that the PSNR of Wavelet transform is the smallest, but of little difference from other algorithms. It represents that the Wavelet transform is like the other denoising methods which have a good denoising ability. However, the EPI of Wavelet transform is the fastest from 1, and it indicates that the Wavelet transform is poor in the edge preservation ability of images. The EPI of Shearlet transform is the nearest to 1. So edge preservation ability of Shearlet transform is very nice and the Shearlet transform also has a higher PSNR. Comprehensive comparison of PSNR and EPI, the Shearlet transform is the best denoising algorithm compared with other methods in this paper.

In order to verify whether the above conclusion has the same result in the actual tree radar B-scan image. This paper applies the Wavelet, Curvelet, Contourlet and Shearlet transform to real tree trunk radar B-scan images. A tree trunk which has an internal decay or void is shown in Fig.13(a). The longest diameter of the trunk is 72 centimeters and the shortest diameter is 52 centimeters. Therefore, the collection diameter is set as 65 centimeters. The radar B-scan image of the trunk is shown in Fig.14(b).

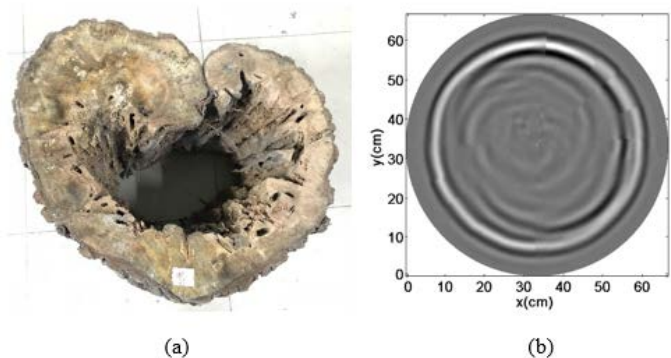


Fig. 12 (a) Tree trunk image, (b) Tree radar B-scan image.

Fig.13 is the denoising effect images of above algorithms. The results in the Fig.13 show that the four denoising methods have improved the visual effects by removing the noise from the tree radar images. In order to compare the denoising effects of various denoising algorithms, this paper performs the difference processing between the denoised effect map and the original B-scan diagram. The difference images are shown in Fig.15.

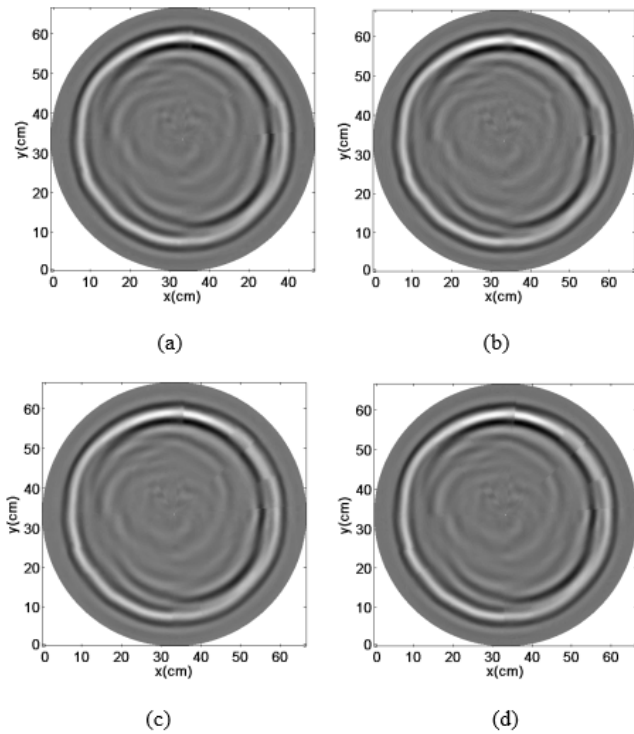


Fig. 13(a) De-noised image of Wavelet transform. (b) De-noised image of Curvelet transform. (c) De-noised image of Contourlet transform. (d) De-noised image of Shearlet transform.

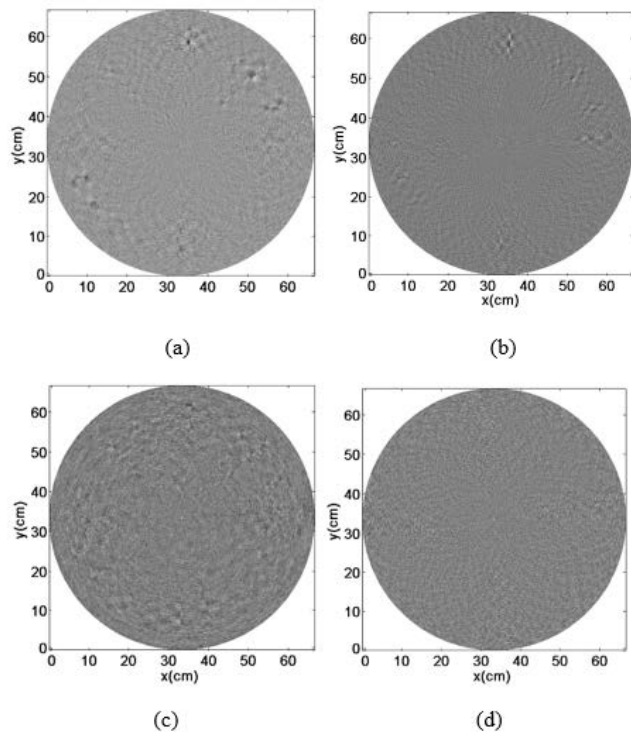


Fig. 14 (a) The difference image of Wavelet transform, (b) The difference image of Curvelet transform, (c) The difference image of Contourlet transform, (d) The difference image of Shearlet transform.

Fig.16(a) is the difference chart of Wavelet transform. It can be seen that the difference chart contains obvious defect feature information. The edges of the difference diagrams of Curvelet transform and Contourlet transform also show some obvious edge feature information. This shows that the Wavelet transform, Curvelet transform and Contourlet transform have removed the defect information after removing the noise of the tree radar B-scan image. However, just the white noise spots appear in the difference map of the Shearlet transform. This shows that the Shearlet transform does not cause the loss of the edge feature information of radar B-scan image, so the Shearlet transform has a better ability to maintain the defect characteristics of tree radar B-scan image.

In order to further evaluate the denoising effects of above denoising algorithms, the PSNR and EPI have been counted and shown in Table 2.

Table 2: The digital results of 4 denoising methods in tree radar B-scan image data.

	Wavelet	Curvelet	Contourlet	Shearlet
PSNR	66.1887	66.8847	66.2966	68.5429
EPI	0.2122	0.2874	0.3447	0.3592

It is observed from Table 2 that the PSNR of Wavelet transform is 66.1887 which is the smallest of the four denoising methods. This indicates that the performance of removing noise of Wavelet transform is the worst. The PSNR of Curvelet transform is 66.8847 which is higher than the Contourlet transform. But the EPI of Contourlet transform is closer to 1 than the EPI of Curvelet transform. It explains that the performance of removing the noise of Curvelet transform is better, but the edge retention is better for Contourlet transform. The Shearlet transform has the highest PSNR compared with other algorithms in this paper and its EPI is also the closest to 1. The result indicates that the Shearlet transform is a more suitable algorithm for tree radar B-scan image.

#### IV. CONCLUSION AND DISCUSSION

This paper uses ground penetrating radar to detect the interior defects of a tree trunks. In view of the low signal to noise ratio of tree radar images and the inconspicuous edge features of defects, in this paper, the multi scale analysis image noise removal algorithms are used to de-noise the tree radar images and extract the characteristics of internal tree defects effectively. Experiments are carried out on forward data and actual tree radar B-scan images. The results show that those algorithms can improve the signal to noise ratio of the tree radar B-scan images without affecting the imaging accuracy and effectively extract and retain the internal defect features of trees meantime. This paper compared the PSNR and EPI of Wavelet, Curvelet, Contourlet and Shearlet transform. The results show that the Shearlet transform has the highest PSNR and the EPI of Shearlet transform also is closer to 1. It can conclude that the Shearlet transform is more suitable for removing noise from tree radar B-scan images.

## REFERENCES

- [1] Colla C. GPR of a timber structural element[C]. International Conference on Ground Penetrating Radar. IEEE, 2010:1-5.
- [2] Martínez-Sala R, Rodríguez-Abad I, Barra R D, et al. Assessment of the dielectric anisotropy in timber using the nondestructive GPR technique[J]. *Construction & Building Materials*, 2013, 38:903-911.
- [3] Li W, Wen J, Xiao Z, et al. Application of Ground-Penetrating Radar for Detecting Internal Anomalies in Tree Trunks with Irregular Contours[J]. *Sensors*, 2018, 18(2):649.
- [4] Xiao Z L, Wen J, Gao L, et al. Method of tree radar signal processing based on Curvelet transform[J]. *Revista Tecnica de la Facultad de Ingenieria Universidad del Zulia*, 2016, 39(7): 243-250.
- [5] Long J, Wang X, Dai D, et al. Denoising of UHF PD signals based on optimised VMD and Wavelet transform[J]. *Iet Science Measurement & Technology*, 2017, 11(6):753-760.
- [6] Ansari R A, Budhhiraju K M. A Comparative Evaluation of Denoising of Remotely Sensed Images Using Wavelet, Curvelet and Contourlet Transforms[J]. *Journal of the Indian Society of Remote Sensing*, 2017, 44(6):1-11.
- [7] Kamble V M, Parlewar P, Keskar A G, et al. Performance evaluation of Wavelet, ridgelet, Curvelet and Contourlet transforms based techniques for digital image denoising[J]. *Artificial Intelligence Review*, 2016, 45(4):509-533.
- [8] Goyal P, Tiwari V M. Application of the continuous Wavelet transform of gravity and magnetic data to estimate sub- basalt sediment thickness[J]. *Geophysical Prospecting*, 2014, 62(1):148-157.
- [9] Kumar R, Singh M. Outer race defect width measurement in taper roller bearing using discrete Wavelet transform of vibration signal[J]. *Measurement Journal of the International Measurement Confederation*, 2013, 46(1):537-545.
- [10] Cieszczyk S, Lawicki T, Miaskowski A. The Curvelet Transform Application to the Analysis of Data Received from GPR Technique[J]. *Elektronika Ir Elektrotechnika*, 2013, 19(6):99-102.
- [11] Tzanis A. The Curvelet Transform in the analysis of 2-D GPR data: Signal enhancement and extraction of orientation-and-scale-dependent information[J]. *Journal of Applied Geophysics*, 2015.
- [12] Terrasse G, Nicolas J M, Trouvé E, et al. Application of the Curvelet transform for pipe detection in GPR images[C], *Geoscience and Remote Sensing Symposium. IEEE*, 2015:4308-4311.
- [13] Satheesh S, Prasad K. Medical Image Denoising Using Adaptive Threshold Based on Contourlet Transform[J]. *Advanced Computing An International Journal*, 2011, 2(2):52-58.
- [14] Guo Q, Dong F, Sun S, et al. Improved Rotating Kernel Transformation Based Contourlet Domain Image Denoising Framework[C]// *Pacific-Rim Conference on Multimedia. Springer International Publishing*, 2013:146-157.
- [15] Yuan Y, Xie L, Zhu Y, et al. SAR image de-noising using local properties analysis and discrete non-separable Shearlet transform[C]// *International Congress on Image and Signal Processing, Biomedical Engineering and Informatics. IEEE*, 2018.
- [16] Wang X, Liu S, Hao C. Application of Shearlet Transform for Suppressing Random Noise in GPR Data[J]. *Journal of Jilin University*, 2017, 47(6):1855-1864.
- [17] Ram I, Elad M, Cohen I. Generalized Tree-Based Wavelet Transform[J]. *IEEE Transactions on Signal Processing*, 2011, 59(9):4199-4209.
- [18] Do M N, Vetterli M. The Contourlet transform: an efficient directional multiresolution image representation.[J]. *IEEE Transactions on Image Processing A Publication of the IEEE Signal Processing Society*, 2005, 14(12):2091-2106.
- [19] Gupta D, Anand R S, Tyagi B. Enhancement of Medical Ultrasound Images Using Multiscale Discrete Shearlet Transform Based Thresholding[C] *International Symposium on Electronic System Design. IEEE Computer Society*, 2012:286-290.
- [20] Mishra M K, Zafar S. Performance Analysis of Probshrink Image Denoising Method Based on its PSNR Value[J] *International Journal of Engineering Innovation & Research*. 2014, 3(1): 62-66.
- [21] Sivakumar R. Denoising of computer tomography images using Curvelet transform[J]. *Journal of Engineering & Applied Sciences*, 2007, 2(1): 21-26.
- [22] Harish K N, Amutha. S, Ramesh B D R. Enhancement of Mammographic Images using Morphology and Wavelet Transform[J]. *International Journal of Computer Technology & Applications*, 2012, 3(1):192-198.